INT. J. REMOTE SENSING, 20 DECEMBER, 2004,
VOL. 25, NO. 24, 5731–5744

Taylor & Francis
Taylor & Francis Group

Mapping snow cover in the pan-Arctic zone, using multi-year (1998–2001) images from optical VEGETATION sensor

X. XIAO*, Q. ZHANG, S. BOLES, M. RAWLINS and B. MOORE III

Institute for the Study of Earth, Oceans and Space, University of New Hampshire, Durham, NH 03833, USA

(*Received 24 March 2003; in final form 13 April 2004*)

Abstract. Timely information on spatial distribution and temporal dynamics of snow cover in the pan-Arctic zone is needed, as snow cover plays an important role in climate, hydrology and ecological processes. Here we report estimates of snow cover in the pan-Arctic zone (north of 45° N) at 1-km spatial resolution and at a 10-day temporal interval over the period of April 1998 to December 2001, using 10-day composite images of VEGETATION sensor onboard Système Pour l'Observation de la Terre (SPOT)-4 satellite. The results show that snow covered area (SCA) in North America (north of 45° N) increased from 1998 to 2001, while SCA in Eurasia (north of 45° N) decreased from 1998 to 2000 but increased in 2001. There were large spatial and temporal variations of snow cover in the pan-Arctic zone during 1998–2001.

1. Introduction

During winter and spring, the land surface in high altitudes, northern temperate and boreal zones is frequently covered by snow. Snow cover is characterized by rapid seasonal changes and large spatial variations, and plays an important role in climate and water resources (Goodison *et al*. 1999, Pielke *et al*. 2000, Groisman and Davies 2001). Variable snow distribution influences the outcomes of simulations of hydrologic and ecosystem processes. The end-of-winter snow distribution is a crucial input to snowmelt hydrology models, including those used for water-resource management (Martinec and Rango 1981, Kane *et al*. 1991, Hartman *et al*. 1999). The problem of realistically representing seasonal snow in atmospheric, hydrologic, and ecological models is made complex because of the numerous snow-related features that display considerable spatial variability at scales below those resolved by the models. A patchy mosaic of snow and vegetation caused by redistribution and snowmelt strongly influences the energy fluxes returned to the atmosphere, and the associated feedbacks that accelerate the melt of remaining snow-covered areas (Shook *et al*. 1993, Essery 1997, Liston and Sturn 1998, Neumann and Marsh 1998, Liston 1999). Seasonal dynamics of snow cover are

*Corresponding author; tel: (603) 8623818, fax: (603) 862-0188, e-mail: xiangming.xiao@unh.edu

International Journal of Remote Sensing
ISSN 0143-1161 print/ISSN 1366-5901 online © 2004 Taylor & Francis Ltd
http://www.tandf.co.uk/journals
DOI: 10.1080/01431160410001719867

related to length and timing of photosynthetic active period of vegetation, and affected net ecosystem exchange of CO_2 between forest ecosystems and the atmosphere (Goulden *et al*. 1996, 1998, Black *et al*. 2000). Snow cover dynamics (accumulation, melting and depletion) have significant implications for atmospheric, hydrologic and ecologic modelling (Liston 1999).

The linkage between snow cover (one of hydrological processes) and biogeochemical processes (CO_2 fluxes and trace gases emissions) takes place at ecosystem to landscape scales. Quantification of CO_2 fluxes and trace gases emissions of terrestrial ecosystems in the pan-Arctic zone has been hampered by lack of geospatial datasets of snow cover at ecosystem- to landscape resolutions (a resolution of a few hundreds of metre to kilometre). At large spatial scales, snow cover detection methods and available snow cover products are primarily based on three groups of space-borne sensors (Chang *et al*. 1987, Rango 1993, Grody and Basist 1996, Cline and Carroll 1999, Tait *et al*. 2000): (1) optical sensors (e.g. Advanced Very High Resolution Radiometer (AVHRR)), (2) passive microwave sensors (e.g. Defense Meteorological Satellite Program (DMSP) Special Sensor Microwave/Imager (SSM/I), Nimbus-7 Scanning Multi-channel Microwave Radiometer (SSMR)) and (3) active synthetic aperture radar (e.g. Radarsat, European Remote Sensing Satellite (ERS)-1/2). To date, large-scale (continental to global) operational mapping and monitoring of snow cover has been largely dependent upon the image data from AVHRR onboard the National Oceanic and Atmospheric Administration (NOAA) meteorological satellites (Robinson *et al*. 1993, Frie and Robinson 1999). The widely-used Northern Hemisphere EASE-Grid snow cover dataset at National Snow and Ice Data Center (NSIDC; Armstrong and Brodzik 2002, http://nsidc.org/) has a coarse spatial resolution (e.g. 25-km grid). Satellite and land surface observations have indicated that snow cover area in the Northern Hemisphere has declined significantly over the last several decades, particularly in the spring season (Groisman *et al*. 1994a, Robinson *et al*. 1995, Brown 2000, Easterling *et al*. 2000).

Recently, a new generation of advanced optical space-borne sensors has successfully been launched (e.g. VEGETATION (VGT) sensor onboard Système Pour l'Observation de la Terre (SPOT)-4 in 1998, Moderate-resolution Imaging Spectroradiometer (MODIS) sensor onboard Earth Observing System (EOS) Terra in 1999). These new sensors have more spectral bands (table 1) and offer much

Table 1. A comparison of spectral bands among SPOT-4 (VGT), NOAA AVHRR, Terra MODIS and Landsat TM optical sensors.

Feature	SPOT-4 VGT (nm)	NOAA AVHRR (nm)	Terra MODIS (nm)	Landsat TM (nm)
Blue	B0 (430–470)		B3 (459–479)	TM1 (450–520)
Green			B4 (545–565)	TM2 (520–600)
Red	B2 (610–680)	CH1 (580–680)	B1 (620–670)*	TM3 (630–690)
	B3 (780–890)	CH2 (725–1100)	B2 (841–876)*	TM4 (760–900)
Near-infrared			B5 (1230–1250)	
	SWIR (1580—1750)		B6 (1628–1652)	TM5 (1550–1750)
Shortwave infrared			B7 (2105–2155)	TM7 (2080–2350)
Spatial resolution	1 km	1 km	250 m*, 500 m	30 m
Revisit time	Daily	Daily	Daily	16-day

*Spectral bands with 250 m spatial resolution.

improved potential for quantifying seasonal dynamics and inter-annual variation of snow cover in the globe at moderate spatial resolutions (e.g. 500 m to 1 km). In order to reduce data volume and have cloud-free images, 10-day composites of VGT images (http://free.vgt.vito.be) and 8-day composites of MODIS images (http://edc.usgs.gov/products/satellite.html) are provided to users for satellite-based studies of land cover classification, vegetation growth, and CO_2 fluxes. Information on snow cover is needed for analysis of those 10-day composites of VGT images and 8-day composites of MODIS images. Recently, significant progress has been made in using images from those advanced optical sensors (VGT, MODIS) for identifying and mapping of snow cover at such a spatial resolution that is comparable with the studies of ecosystems and landscape processes (Hall *et al*. 2002, Xiao *et al*. 2002a). In this study, our specific objective is twofold: (1) to develop a multi-year dataset of snow cover at 1-km spatial resolution over the period of April 1998 to December 2001, using the 10-day composites of VGT (VGT-S10) image data; and (2) to further document the potential of VGT sensor for identification and mapping of snow cover at large spatial scales. The resultant snow cover dataset will help quantify seasonal dynamics and inter-annual variations of snow cover in the pan-Arctic zone from April 1998 to December 2001, and could also be used to support other analyses of 10-day composites of VGT images, for instance, forest classification and vegetation indices (Xiao *et al*. 2002b, 2003).

2. Data and methods

2.1. *Multi-temporal images from the VGT sensor*

The VGT instrument has four spectral bands (table 1). The blue band is primarily used for atmospheric correction. The short-wave infrared (SWIR) band is sensitive to soil moisture, vegetation cover and leaf moisture content, and can improve the discrimination of vegetation and other land covers. With a swath width of 2250 km, VGT provides daily coverage of the globe at 1-km spatial resolution. Multi-year VGT images have been accumulated since April 1998. The VGT sensor uses the same geometric reference system and has identical spectral bands to the SPOT High Resolution Visible and Infrared sensor to facilitate multi-scale interpretation.

Three standard VGT products are available to users: VGT-P (physical product), VGT-S1 (daily synthesis product) and VGT-S10 (10-day synthesis product). The spectral bands in the VGT-S1 products are estimates of ground surface reflectance, as atmospheric corrections for ozone, aerosols and water vapour have been applied to the VGT-P images using the simplified method for atmospheric correction algorithm (Rahman and Dedieu 1994). VGT-S10 data are generated by selecting the VGT-S1 pixels that have the maximum Normalized Difference Vegetation Index (NDVI) values within a 10-day period, thus minimizing the effect of cloud cover and variability in atmospheric optical depth. There are three 10-day composites for one month: days 1–10, days 11–20 and day 21 to the last day of a month. Global VGT-S10 data are freely available to the public (http://free.vgt.vito.be). The spatial domain of the global VGT-S10 data ranges from 56° S to 75° N, which results in a data void region around the North Pole throughout a year. In addition, VGT sensor had no observations at very high latitudes in late-autumn/winter/early-spring seasons, because of no sunlight illumination at local passing times of satellite. The resultant data void region (for VGT-S10 data) varied in size over time and thus has some implications on estimates of snow cover area

during late-autumn/winter/early-spring seasons in the pan-Arctic zone. The maximum snow cover area in early spring season (March) could be used as an approximate estimate of maximum snow cover area in a year, because air temperature in that period (March) could be still too cold for snow cover at very high latitudes to melt.

2.2. *Description of the algorithms for identifying snow cover*

Snow and ice cover have very high spectral reflectance values in the visible wavelengths (400–700 nm), but have low reflectance values in the SWIR wavelengths (1550–1750 nm). Among the four types of snow and ice cover with different grain sizes, the differences in spectral reflectance are relatively small in visible wavelengths but large in SWIR wavelengths (figure 1). The Normalized Difference Snow Index (NDSI), which is calculated as a normalized difference between the spectral reflectance values of green and SWIR bands, was proposed to identify and map snow cover (Hall *et al.* 1995, 1998). For Landsat Thematic Mapper (TM) data, NDSI is calculated using the green band (TM2) and SWIR band (TM5):

$$\mathrm{NDSI_{TM}} = (\mathrm{TM2} - \mathrm{TM5})/(\mathrm{TM2} + \mathrm{TM5}) \quad (1)$$

Hall *et al.* (1995, 1998) used NDSI threshold values for snow cover mapping. If a pixel had NDSI $\geqslant 0.40$ and near-infrared (NIR) reflectance > 0.11, the pixel was classified as snow/ice cover. This NDSI-based algorithm (SNOMAP) is used to generate the MODIS standard product for snow cover at the global scale (Hall *et al.* 1995, 2002).

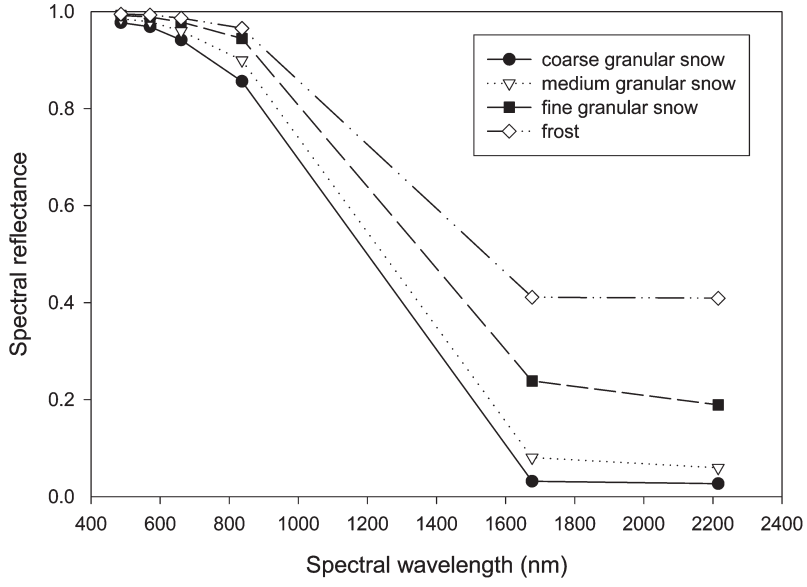

Figure 1. Spectral reflectance of four types of snow and ice cover, as measured according to Landsat 5 TM spectral bandwidth. It is based upon the spectral library for snow and ice covers from the Johns Hopkins University. The spectral library and spectral re-sampling algorithm are available in the commercial ENVI software (Research System Inc.), and spectral re-sampling of the spectral library was conducted, using Landsat 5 TM spectral bandwidth.

Other studies have suggested that red wavelengths are useful for identifying snow and ice cover (Boresjö Bronge and Bronge 1999, Sidjak and Wheate 1999). Using Landsat TM data and ground radiometer measurements to classify ice and snow-type in the eastern Antarctic, Boresjö Bronge and Bronge (1999) found that the RED/NIR (TM3/TM4) ratio is a simple tool for distinguishing between blue-ice and snow, and the RED/SWIR (TM3/TM5) ratio is a useful tool for quantifying snow grain-size variations. The Normalized Difference Snow/Ice Index (NDSII), which is calculated as a normalized difference between red and SWIR bands, was proposed (Xiao *et al*. 2001). For Landsat TM data, NDSII is calculated as:

$$\mathrm{NDSII_{TM}} = (\mathrm{TM3} - \mathrm{TM5})/(\mathrm{TM3} + \mathrm{TM5}) \tag{2}$$

A comparison study of NDSI and NDSII was conducted, using one Landsat TM image in the Qinghai-Tibet plateau of China (Xiao *et al*. 2001). Spatial data of NDSI and NDSII from the Landsat TM image showed that NDSII values were highly correlated with NDSI values. To determine whether a pixel is covered by snow/ice or not, the same thresholds proposed by Hall *et al*. (1995, 1998) were used. If a pixel had NDSII $\geqslant 0.40$ or NDSI $\geqslant 0.40$ and a NIR reflectance value > 0.11, the pixel was classified as snow/ice. The results showed that the NDSI- and NDSII-based algorithms gave similar estimates of area and spatial distribution of snow/ice cover (Xiao *et al*. 2001). Because the VGT sensor has red and SWIR bands equivalent to Landsat TM (table 1), it has the potential for identifying and mapping snow cover at large spatial scales. For VGT data, NDSII is calculated using surface reflectance values of red (B2) and SWIR bands:

$$\mathrm{NDSII_{VGT}} = (\mathrm{RED} - \mathrm{SWIR})/(\mathrm{RED} + \mathrm{SWIR}) \tag{3}$$

The VGT-specific $\mathrm{NDSII_{vgt}}$ (equation (3)) was first used to identify and map snow/ice cover in the Qinghai-Tibet Plateau of China, using 10-day composite VGT data from March 1999 to November 1999 (Xiao *et al*. 2002a). Using the snow/ice identification thresholds (NDSII $\geqslant 0.40$ and NIR > 0.11) developed in an earlier study (Xiao *et al*. 2001), the VGT NDSII algorithm provided reasonable estimates of the spatial and temporal dynamics of snow/ice cover in the entire Qinghai-Tibet Plateau (Xiao *et al*. 2002a).

In this study, we downloaded VGT-S10 data for North America, Europe and North Asia over the period of 1–10 April 1998 to 21–31 December 2001 (a total of 135 observations in the time series data at 10-day interval). The data of these three regions were combined together and subset to cover the pan-Arctic zone (north of 45° N to 75° N). Note that as Sun illumination in high latitudes changes over seasons, the land area that is observed by optical VGT sensor also changes accordingly, with the least amount of observations in winter season and the largest amount of observations in summer season in the pan-Arctic zone. We first calculated $\mathrm{NDSII_{VGT}}$ for all the VGT-S10 composites during April 1998–December 2001, and then applied the same decision thresholds (NDSII $\geqslant 0.40$ and NIR > 0.11) used in the earlier studies (Xiao *et al*. 2001, 2002a) to identify and map snow cover. The VGT-S10 product provides cloud flag in status map file, and we excluded those cloudy pixels in calculation of $\mathrm{NDSII_{VGT}}$ and snow cover.

3. Results

There were distinct seasonal dynamics of snow-covered area (SCA) in the pan-Arctic zone (figure 2(*a*)). Conventional definitions of the four seasons are used

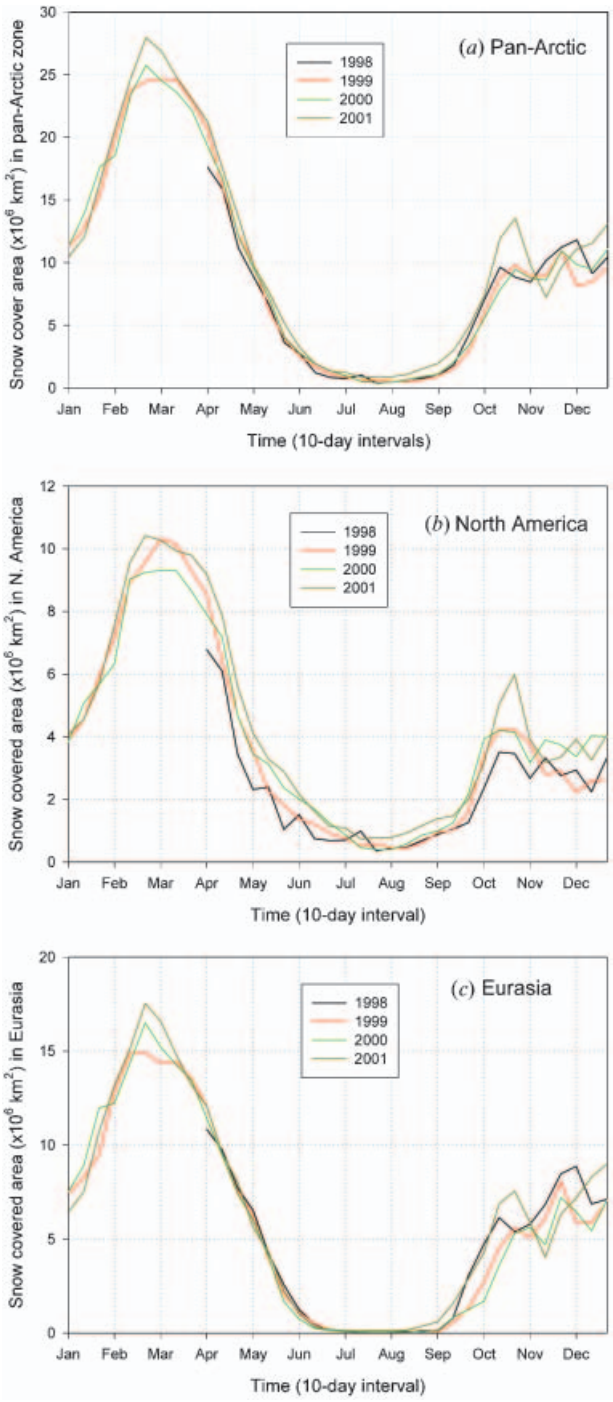

Figure 2. Seasonal dynamics and inter-annual variations of snow cover in the pan-Arctic zone (45° N to 72° N) during April 1998 to December 2001: (*a*) SCA in the pan-Arctic zone, (*b*) SCA in North America, and (*c*) SCA in Eurasia. Note that there are no observations from optical VGT sensor during winter for a large portion of high latitudes because of no Sun illumination; SCA was underestimated in winter season. The largest SCA in early spring can be used to estimate SCA in the winter season.

here: winter (December, January, February), spring (March, April, May), summer (June, July, August) and autumn (September, October, November). During mid-summer, SCA reached its lowest values within a year. SCA increased gradually from late September, as the autumn and winter seasons approach. SCA was generally highest during late winter and early spring. As the spring season progressed, air temperature increased and SCA declined gradually. While the seasonality of SCA in North America (figure 2(*c*)) is generally similar to that in Eurasia (figure 2(*b*)), snowmelt tends to occur slightly earlier in Eurasia than in North America in the spring (figure 2(*b*), (*c*)).

There were only slight inter-annual variations of SCA for the pan-Arctic zone during 1998–2001 (figure 2(*a*)). SCA in the pan-Arctic zone increased in late spring during 1998–2001 but decreased in autumn during 1998–2000. Spring and autumn seasons of year 2001 had the largest SCA in the pan-Arctic zone. Geographically, inter-annual variation of SCA differed between North America and Eurasia (figure 2(*b*), (*c*)). The SCA in North America (north of 45° N) increased slightly from 1998 to 2001, in both late spring to early summer and autumn season (figure 2(*b*)). In contrast, SCA in Eurasia had a slight decrease from 1998 to 2001 in spring season, and a relatively large decline from 1998 to 2000 in autumn season (figure 2(*c*)). The SCA in Eurasia was higher in autumn of 2001 than the other three years.

We calculated SCA frequency (number of observations as snow cover within a year) for individual image pixels and generated maps to illustrate the spatial distribution of snow cover (figure 3). In general, the spatial distributions of SCA frequency agreed relatively well among years (1998–2001). The large SCA in Eurasia in 2001 (figure 2(*c*)) was mostly attributed to more snow cover in the eastern part of Eurasia, including Mongolian Plateau and the north-eastern part of the Far East of Russia (figure 3). The high SCA frequency occurred in mountains (e.g. Rocky Mountains in western North America). The spatial distribution of snow/ice cover was strongly influenced by topography (Cline 1997, Cline *et al.* 1998, Konig and Sturn 1998). We downloaded the Global Land One-kilometer Base Elevation (GLOBE) digital elevation dataset, which was released by the NOAA National Geophysical Data Center (NDGC) in 1999 (the website http://www.ngdc.noaa.gov/). The digital elevation model (DEM) dataset has a spatial resolution of 30 arc second (figure 4). The DEM dataset for the pan-Arctic zone was co-registered with the VGT-derived snow cover dataset. Visual comparison of the DEM and the snow cover datasets revealed a strong spatial agreement between snow cover and topographical features (figures 3, 4).

4. Discussion

The resultant multi-year VGT snow cover dataset will supplement other existing multi-year snow cover datasets, such as those derived from AVHRR images (Ramsay 1998, Cline and Carroll 1999, Armstrong and Brodzik 2002). A simple comparison between the VGT snow cover dataset and the Northern Hemisphere Equal Area Scalable Earth (EASE)-Grid snow cover dataset (Armstrong and Brodzik 2002) archived at the National Snow and Ice Data Center (the snow cover dataset was called NSIDC version 2 in this study) was conducted (figure 5). For the NSIDC version 2 snow cover dataset (3 October 1966–24 June 2001), snow cover extent is based on the digital NOAA-National Environmental Satellite, Data and Information Service (NESDIS) Weekly Northern Hemisphere Snow Charts, revised by D. Robinson (Rutgers University) and regridded to the EASE-Grid (25-km

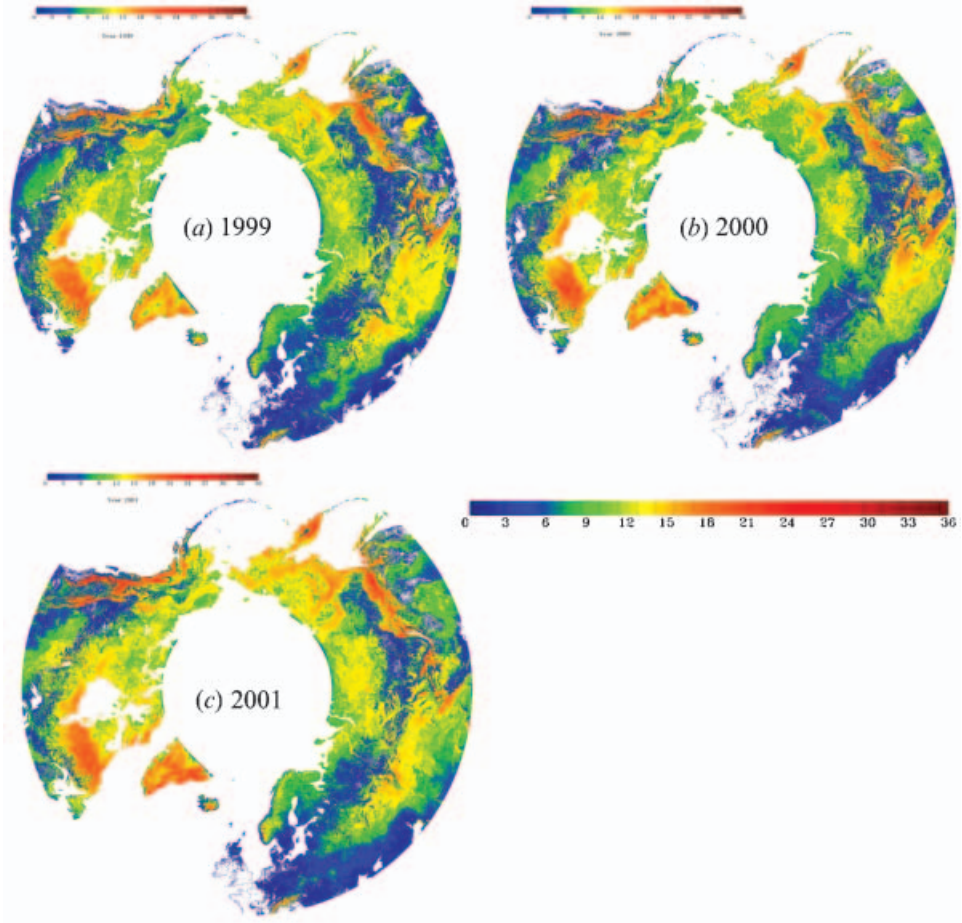

Figure 3. The spatial distribution of snow cover frequency (number of observations as snow cover within a year) in the pan-Arctic zone (45° N to 72° N). There are 36 10-day composites of VGT images in a year: (*a*) 1 January–31 December 1999, (*b*) 1 January–31 December 2000, and (*c*) 1 January–31 December 2001. Note that here we do not include the snow cover frequency map of 1998, as SPOT-4 VGT sensor was launched in March 1998 and VGT-S10 data are available only for the period April–December 1998.

equal-area grid). The original NOAA-NESDIS weekly snow charts are derived from the manual interpretation of AVHRR, Geostationary Satellite (GOES), and other visible-band satellite data (Armstrong and Brodzik 2002). The 1-km VGT-derived snow cover data were aggregated to 25-km EASE-Grid. While the seasonal dynamics of snow cover were similar, the total SCA between the VGT dataset and NSIDC version 2 dataset differed significantly over seasons, particularly in winter. The differences in total SCA could be attributed to a few sources. First of all, as shown in figure 6, there are some differences in spatial coverage between the VGT-S10 reflectance dataset (only reaching 75° N during summer) and the NSIDC version 2 dataset (covering the entire Arctic Circle). Secondly, the VGT-S10 reflectance data had no observations for very high latitudes during the winter season because of no sunlight illumination; it resulted in underestimation of snow cover area during winter and early spring seasons. Thirdly, the NSIDC version 2

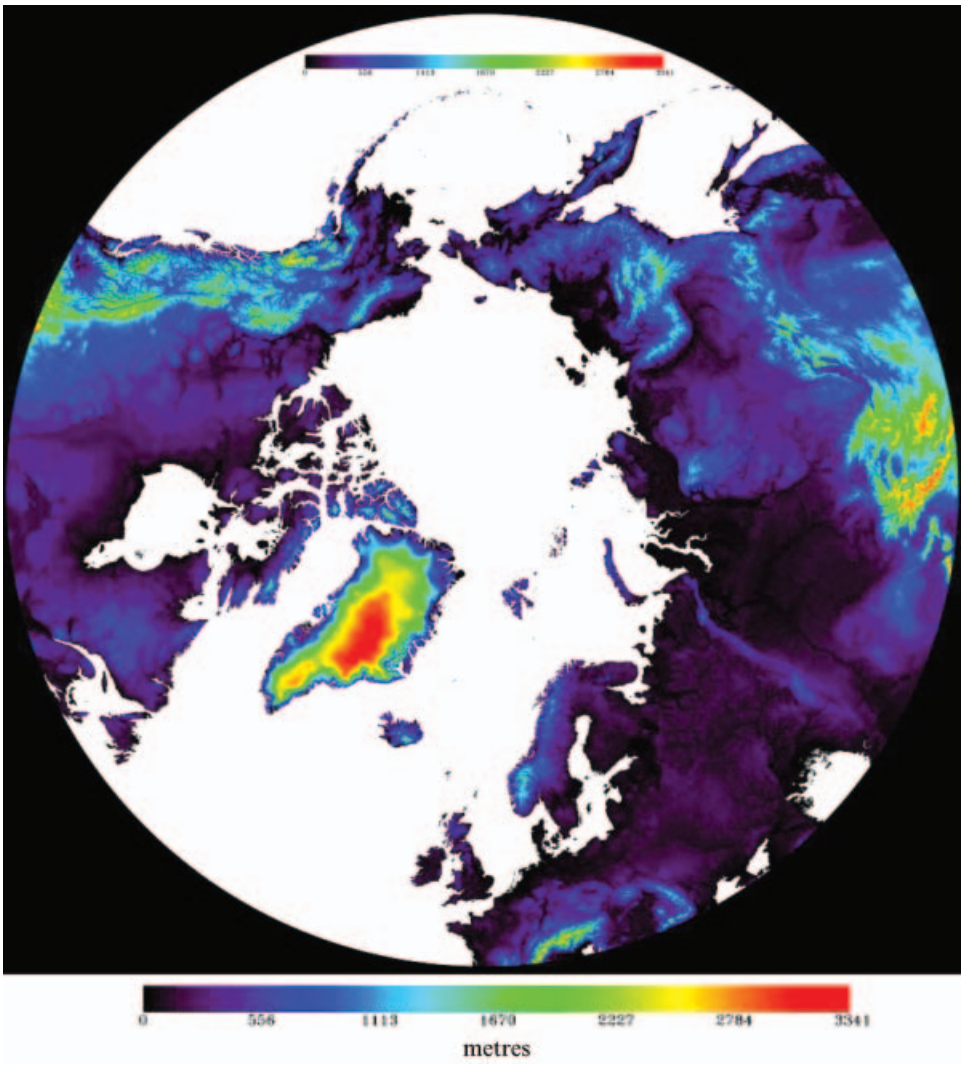

Figure 4. Digital elevation model for the pan-Arctic zone. Elevation ranges from 0 to 3341 m, as shown in the colour legend.

snow cover dataset is a binary map (presence or no presence map) at 25-km grid. If a grid cell was assigned as snow cover, the entire grid cell area ($25 \times 25\,km^2$) is assumed to be snow cover, without considering actual percentage fraction of snow cover within the grid cell (ranging from 50% to 100%), which is likely to result in overestimation of snow cover area. In contrast, the VGT-derived snow cover dataset has a spatial resolution of 1 km, and is aggregated to calculate percentage fraction of snow cover within individual EASE-Grid cells (25-km spatial resolution). Fourthly, since the 10-day composites of VGT data were used in this study, it is likely that the compositing method used in generating 10-day composites (selecting an observation of maximum NDVI value within a 10-day period) might miss some short-duration (less than 10 days) snow events, particularly in late spring and early autumn seasons, when land surface temperature

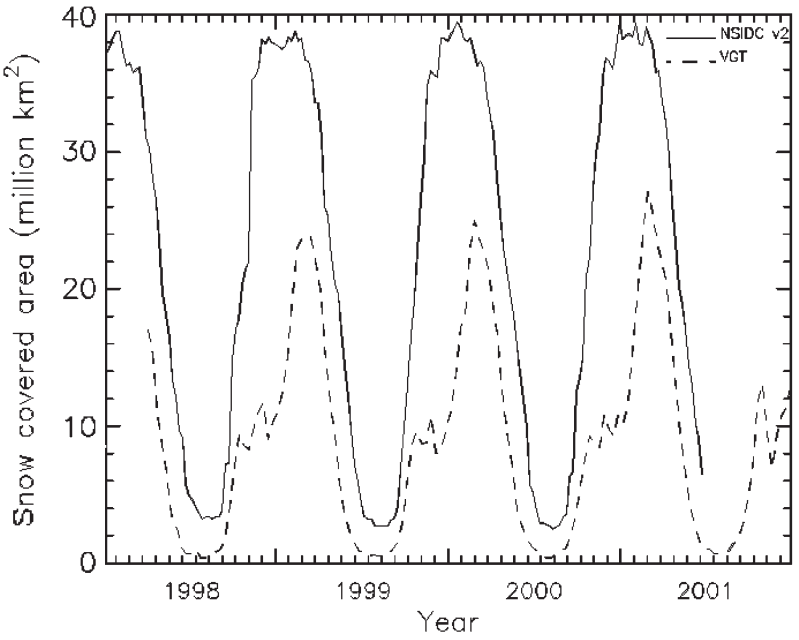

Figure 5. A comparison of total snow covered area (SCA) between the NSIDC Northern Hemisphere Weekly EASE-Grid snow cover dataset (Armstrong and Brodzik 2002) and the VGT-derived snow cover dataset for the pan-Arctic zone (45° N and poleward).

is warm and snow may melt within a few days. There also existed some differences in spatial distribution of snow cover between the NSIDC version 2 snow cover dataset and the VGT-derived snow cover dataset; for instance, during early April 2000, snow covered area in the VGT-derived snow cover dataset was much less than the NSIDC snow cover dataset in the southern part of the pan-Arctic zone (figure 6), when using the threshold of $\geqslant 50\%$ snow cover within individual EASE-Grid cells, which was used in generating the NSIDC Northern Hemisphere Weekly EASE-Grid snow cover dataset (Armstrong and Brodzik 2002).

A number of studies have indicated that there is a strong linkage between Eurasian snow cover and climate (Douville and Royer 1996, Clark *et al.* 1999, Cohen and Entekhabi 1999). North Atlantic Oscillation (NAO) is the primary control factor for winter climate variability in the North Atlantic region ranging from central North America to Europe and much into northern Asia. The positive (or negative) NAO index phases were closely related to winter climate and varied over years (Hurrell 1995). Year 1998, 1999 and 2000 had positive NAO index, while year 2001 had negative NAO index. In those years with positive NAO index, Europe had warm and wet winters, but northern Canada and Greenland had cold and dry winter, and the eastern US experienced mild and wet winter conditions. In those years with negative NAO index, the US east coast experienced more cold air outbreaks and hence snowy weather condition (http://www.cgd.ucar.edu/~jhurrell/nao.html). Snow cover affected heat balance and spring temperature at continental scale (Groisman *et al.* 1994b, Groisman and Davies 2001). Therefore, observed variations of snow cover during 1998–2001 in the pan-Arctic zone (figure 3) may have impacts on climate in Eurasia and North America.

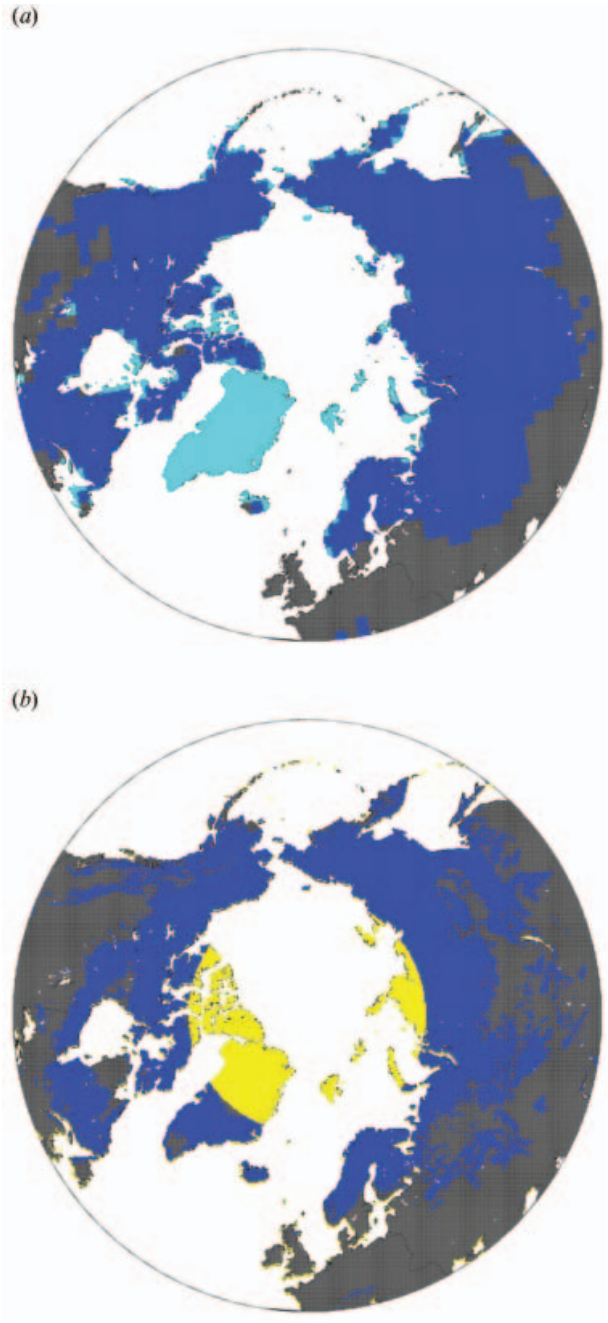

Figure 6. A comparison of spatial distribution of snow cover between the NSIDC Northern Hemisphere Weekly EASE-Grid snow cover dataset (Armstrong and Brodzik 2002) 3–9 April 2002 (*a*) and the VGT-derived snow cover dataset 1–10 April 2002 (*b*) for the pan-Arctic zone (45° N and poleward). The 1-km VGT snow cover dataset was aggregated by calculating the percentage fraction of snow cover within individual EASE-Grid cells (25-km spatial resolution). Colour legend is as follows: EASE-Grid cells with snow ($\geqslant 50\%$ of grid cell is snow covered) in blue, and without snow ($< 50\%$ snow) in grey. Yellow colour in (*a*) represents no data (data void region throughout a year) in the VGT-S10 images.

It is important to note that one of the major advantages of the VGT-derived snow cover dataset is the spatial resolution (1 km), in comparison with other coarse resolution snow cover datasets (e.g. NSIDC Northern Hemisphere Weekly EASE-Grid snow cover dataset (Armstrong and Brodzik 2002)), as analyses of the linkage between hydrological process (e.g. snow cover) and biogeochemical process (e.g. CO_2 fluxes) of terrestrial ecosystems require temporally and spatially consistent datasets resolved at such a spatial resolution (e.g. hundreds of metres to kilometres) that is closely relevant to ecosystem and landscape processes. Earlier studies (Xiao *et al*. 2001, 2002a) and this study have demonstrated the potential of optical VGT sensor for identification and mapping of snow cover at large spatial scales. As more VGT images are available in the near future (from VGT sensors onboard SPOT-4 satellite and SPOT-5 satellite), the multi-year VGT-based dataset of snow cover at 1-km spatial resolution and 10-day temporal resolution is likely to improve simulations of climate, hydrological and ecological processes in the pan-Arctic zone.

Acknowledgments

This study was supported by the NASA Earth Observing System (EOS) Interdisciplinary Science (IDS) program (NAG5-6137, NAG5-10135). We thank anonymous reviewers for their comments and suggestions on the earlier version of the manuscript.

References

ARMSTRONG, R. L., and BRODZIK, M. J., 2002, Northern Hemisphere EASE-Grid weekly snow cover and sea ice extent version 2. National Snow and Ice Data Center, Boulder, CO, USA.

BLACK, T. A., CHEN, W. J., BARR, A. G., ARAIN, M. A., CHEN, Z., NESIC, Z., HOGG, E. H., NEUMANN, H. H., and YANG, P. C., 2000, Increased carbon sequestration by a boreal deciduous forest in years with a warm spring. *Geophysical Research Letters*, **27**, 1271–1274.

BORESJÖ BRONGE, L. B., and BRONGE, C., 1999, Ice and snow-type classification in the Vestfold Hill, East Antarctic, using Landsat TM data and ground radiometer measurements. *International Journal of Remote Sensing*, **20**, 225–240.

BROWN, R. D., 2000, Northern Hemisphere snow cover variability and change: 1915–97. *Journal of Climate*, **13**, 2339–2355.

CHANG, A., FOSTER, J. L., and HALL, D. K., 1987, Nimbus-07 SMMR derived global snow cover parameters. *Annals of Glaciology*, **9**, 39–44.

CLARK, M. P., SERREZE, M. C., and ROBINSON, D. A., 1999, Atmospheric controls on Eurasian snow extent. *International Journal of Climatology*, **19**, 27–40.

CLINE, D. W., 1997, Effects of seasonality of snow accumulation and melt on snow surface energy exchanges at a continental alpine site. *Journal of Applied Meteorology*, **36**, 32–51.

CLINE, D. W., and CARROLL, T. R., 1999, Operational automated production of daily, high-resolution, cloud-free snow cover maps of the continental U.S. *Journal of Geophysical Research*, **104**, 19 631–19 644.

CLINE, D. W., BALES, R. C., and DOZIER, J., 1998, Estimating the spatial distribution of snow in mount basins using remote sensing and energy balance modeling. *Water Resources Research*, **34**, 1275–1285.

COHEN, J., and ENTEKHABI, D., 1999, Eurasian snow cover variability and Northern Hemisphere climate predictability. *Geophysical Research Letters*, **26**, 345–348.

DOUVILLE, H., and ROYER, J. F., 1996, Sensitivity of the Asian summer monsoon to an anomalous Eurasian snow cover within the Meteo-France GCM. *Climate Dynamics*, **12**, 449–466.

EASTERLING, D. R., KARL, T. F., GALLO, K. P., ROBINSON, D. A., TRENBERTH, K. E., and DAI, A., 2000, Observed climate variability and change of relevance to the biosphere. *Journal of Geophysical Research*, **105**, 20 101–20 114.

ESSERY, R. L., 1997, Modeling fluxes of momentum, sensible heat and latent heat over heterogeneous snow cover. *Quarterly Journal of The Royal Meteorological Society*, **123**, 1867–1883.

FREI, A., and ROBINSON, D. A., 1999, Northern Hemisphere snow extent: regional variability 1972–1994. *International Journal of Climatology*, **19**, 1535–1560.

GOODISON, B. E., BROWN, R. D., and CRANE, R. G., 1999, Cryospheric systems. In *EOS Science Plan: The State of Science in the EOS Program*, edited by M. D. King (NASA), pp. 261–307.

GOULDEN, M. L., MUNGER, J. W., FAN, S. M., DAUBE, B. C., and WOFSY, S. C., 1996, Exchange of carbon dioxide by a deciduous forest: response to interannual climate variability. *Science*, **271**, 1576–1578.

GOULDEN, M. L., WOFSY, S. C., HARDEN, J. W., TRUMBORE, S. E., CRILL, P. M., GOWER, S. T., FRIES, T., DAUBE, B. C., FAN, S. M., SUTTON, D. J., BAZZAZ, A., and MUNGER, J. W., 1998, Sensitivity of boreal forest carbon balance to soil thaw. *Science*, **279**, 214–217.

GRODY, N. C., and BASIST, A. N., 1996, Global identification of snow cover using SSM/I measurements. *IEEE Transactions on Geoscience and Remote Sensing*, **34**, 237–249.

GROISMAN, P. Y., and DAVIES, T. D., 2001, Snow cover and the climate system. In *Snow Ecology*, edited by J. G. Jones, J. W. Pomeroy, D. A. Walker and R. W. Hoham (New York: Cambridge University Press) pp. 1–44.

GROISMAN, P. Y., KARL, T. R., KNIGHT, R. W., and STENCHIKO, G. L., 1994a, Change of snow cover, temperature, and radiative heat balance over the Northern Hemisphere. *Journal of Climate*, **7**, 1633–1656.

GROISMAN, P. Y., KARL, T. R., and KNIGHT, R. W., 1994b, Observed impact of snow cover on the heat balance and the rise of continental spring temperature. *Science*, **263**, 198–200.

HALL, D. K., RIGGS, G. A., and SALOMONSON, V. V., 1995, Development of methods for mapping global snow cover using moderate resolution imaging spectroradiometer data. *Remote Sensing of Environment*, **54**, 127–140.

HALL, D. K., FOSTER, J. L., VERBYLA, D. L., and KLEIN, A. G., 1998, Assessment of snow cover mapping accuracy in a variety of vegetation cover densities in central Alaska. *Remote Sensing of Environment*, **66**, 129–137.

HALL, D. K., RIGGS, G. A., SALOMONSON, V. V., DIGIROLAMO, N. E., and BAYR, K. J., 2002, MODIS snow-cover products. *Remote Sensing of Environment*, **83**, 181–194.

HARTMAN, M. D., BARON, J. S., LAMMERS, R. B., CLINE, D. W., BAND, L. E., LISTON, G. E., and TAGUE, C., 1999, Simulations of snow distribution and hydrology in a mountain basin. *Water Resources Research*, **35**, 1587–1603.

HURRELL, J. W., 1995, Decadal trends in the North Atlantic Oscillation: regional temperature and precipitation. *Science*, **269**, 676–679.

KANE, D. L., HINZMAN, L. D., BENSON, C. S., and LISTON, G. E., 1991, Snow hydrology of a headwater Arctic basin 1. Physical measurement and process studies. *Water Resources Research*, **27**, 1099–1109.

KONIG, M., and STURN, M., 1998, Mapping snow distribution in the Alaskan Arctic using air photos and topographic relationships. *Water Resources Research*, **34**, 3471–3483.

LISTON, G. E., 1999, Interrelationships among snow distribution, snowmelt, and snow cover depletion: implications for atmospheric, hydrologic, and ecologic modeling. *Journal of Applied Meteorology*, **38**, 1474–1487.

LISTON, G. E., and STURN, M., 1998, A snow transport model for complex terrain. *Journal of Glaciology*, **44**, 498–516.

MARTINEC, J., and RANGO, A., 1981, Areal distribution of snow water equivalent evaluated by snow cover monitoring. *Water Resources Research*, **17**, 1480–1488.

NEUMANN, N., and MARSH, P., 1998, Local advection of sensible heat in the snowmelt landscape of Arctic tundra. *Hydrological Processes*, **12**, 1547–1560.

PIELKE, R. A., LISTON, G. E., and ROBOCK, A., 2000, Insolation-weighted assessment of Northern Hemisphere snow cover and sea-ice variability. *Geophysical Research Letters*, **27**, 3061–3064.

RAHMAN, H., and DEDIEU, G., 1994, SMAC: a simplified method for atmospheric correction of satellite measurements in the solar spectrum. *International Journal of Remote Sensing*, **15**, 123–143.

RAMSAY, B., 1998, The interactive multisensor snow and ice mapping system. *Hydrological Processes*, **12**, 1537–1546.

RANGO, A., 1993, Snow hydrology processes and remote sensing. *Hydrological Processes*, **7**, 121–138.

ROBINSON, D. A., DEWEY, K. F., and HEIM, R. R., 1993, Global snow cover monitoring: an update. *Bulletin of the American Meteorological Society*, **74**, 1689–1696.

ROBINSON, D. A., FREI, A., and SERREZE, M. C., 1995, Recent variations and regional relationships in Northern Hemisphere snow cover. *Annals of Glaciology*, **21**, 71–76.

SHOOK, K., GRAY, D. M., and POMEROY, J. W., 1993, Temporal variation in snow cover area during snowmelt in prairie and alpine environments. *Nordic Hydrology*, **24**, 183–198.

SIDJAK, R. W., and WHEATE, R. D., 1999, Glacier mapping of the Illecillewaet icefield, British Columbia, Canada, using Landsat TM and digital elevation data. *International Journal of Remote Sensing*, **20**, 273–284.

TAIT, A. B., HALL, D. K., FOSTER, J. L., and ARMSTRONG, R. L., 2000, Utilizing multiple datasets for snow-cover mapping. *Remote Sensing of Environment*, **72**, 111–126.

XIAO, X. M., SHEN, Z. X., and QIN, X. G., 2001, Assessing the potential of VEGETATION sensor data for mapping snow and ice cover: a Normalized Difference Snow and Ice Index. *International Journal of Remote Sensing*, **22**, 2479–2487.

XIAO, X., MOORE, B., QIN, X., SHEN, Z., and BOLES, S., 2002a, Large-scale observations of alpine snow and ice cover in Asia: using multi-temporal VEGETATION sensor data. *International Journal of Remote Sensing*, **23**, 2213–2228.

XIAO, X., BOLES, S., LIU, J. Y., ZHUANG, D. F., and LIU, M. L., 2002b, Characterization of forest types in Northeastern China, using multi-temporal SPOT-4 VEGETATION sensor data. *Remote Sensing of Environment*, **82**, 335–348.

XIAO, X., BRASWELL, B., ZHANG, Q., BOLES, S., FROLKING, S., and MOORE, B., 2003, Sensitivity of vegetation indices to atmospheric aerosols: continental-scale observations in Northern Asia. *Remote Sensing of Environment*, **84**, 385–392.